Energy-dispersive XAFS study on the decarbonylation process of $Mo(CO)_6$ in NaY zeolite

Aritomo Yamaguchi [a], Akane Suzuki [a], Takafumi Shido [a], Yasuhiro Inada [b], Kiyotaka Asakura [c], Masaharu Nomura [d] and Yasuhiro Iwasawa [a,*]

[a] *Department of Chemistry, Graduate School of Science, the University of Tokyo, Hongo, Bunnkyo-ku, Tokyo 113-0033, Japan*
E-mail: iwasawa@chem.s.u-tokyo.ac.jp
[b] *Research Center for Materials Science, Nagoya University, Nagoya 464-8602, Japan*
[c] *Catalysis Research Center, Hokkaido University, Kita-ku, Sapporo 060-0811, Japan*
[d] *Photon Factory, Institute of Materials Structure Science, KEK, Ibaraki 305-0801, Japan*

Received 11 September 2000; accepted 27 November 2000

The temperature-programmed decarbonylation process of $Mo(CO)_6$ in NaY zeolite was studied by means of a time-resolved energy-dispersive XAFS method. The XANES analysis demonstrated that the decarbonylation proceeded by two successive steps via a stable intermediate which existed between 440 and 490 K. The curve fitting analysis of the EXAFS data revealed that the intermediate was a molybdenum monomer subcarbonyl species $Mo(CO)_3(O_L)_3$ coordinated by three CO ligands and three oxygen atoms of zeolite framework (O_L). Molybdenum dimer subcarbonyl species were not observed. This study demonstrated that the DXAFS technique is a powerful method to study the dynamic behavior of the Mo carbonyl species during decarbonylation process.

KEY WORDS: energy-dispersive XAFS; $Mo(CO)_6$ in NaY; molybdenum subcarbonyl species; decarbonylation; structure analysis; time-resolved spectroscopy

1. Introduction

The transformation of a metal complex into an active metal species on inorganic oxides in a controllable manner is a key issue in developing efficient catalytic systems containing metal sites regulated on a molecular level [1–3]. Especially zeolites have been demonstrated to provide highly dispersed metal species [4,5]. $Mo(CO)_6$ is often used to prepare highly dispersed Mo species in zeolites, because $Mo(CO)_6$ is readily decarbonylated to produce Mo species in the channels of zeolites [6–8]. The decomposition behavior of Mo carbonyl species encaged in zeolites has been studied by IR [9–13], temperature-programmed decomposition (TPD) [14,15], and ESR [16] techniques. Several molybdenum subcarbonyl species such as $Mo(CO)_3$, $Mo(CO)_4$, $Mo_2(CO)_6$, and $Mo_2(CO)_8$ have been proposed based on the IR spectra [17–19]. As the IR data do not give direct information on the Mo structure, however, the proposed species are not conclusive or consistent.

On the other hand, XAFS (X-ray absorption fine structure) is a powerful tool to elucidate the local structures of both crystalline and non-crystalline materials such as supported metal catalysts [20]. For this reason XAFS has been applied to determination of the structure of Mo species in Y zeolite. Okamoto et al. investigated the structure of Mo subcarbonyl species in Y zeolite using EXAFS (extended X-ray absorption fine structure) and claimed that $Mo(CO)_3(O_L)_3$ (O_L: zeolite framework oxygen atom) was a stable subcarbonyl species formed by thermal decarbonylation [21]. Asakura et al. also studied the structure of the molybdenum species produced by saturated adsorption of $Mo(CO)_6$ at room temperature and subsequent decarbonylation at 573 K, and found that molybdenum oxycarbide dimer $Mo_2(C)O_x$ was formed in the supercage of NaY zeolite [6,7].

However, dynamic structural changes of the molybdenum species during the thermal decarbonylation have not been studied in detail, and the following questions remain unanswered:

(i) Does the $Mo(CO)_3(O_L)_3$ convert into $Mo_2(C)O_x$ by evacuation at 573 K, or are these species formed through different paths?

(ii) Do the species that were suggested by IR really exist?

We measured energy-dispersive XAFS (DXAFS) to answer the questions. DXAFS is an experimental method to acquire XAFS data in a short period using a bent crystal polychromator and a position-sensitive detector [20,22–24]. The X-rays in the whole energy range are monitored simultaneously and the data acquisition time is about 1 s in the present study. It is expected that the DXAFS technique will provide useful information on the dynamic structural change of the Mo species during temperature-programmed decarbonylation of $Mo(CO)_6$/NaY.

* To whom correspondence should be addressed.

1011-372X/01/0200-0203$19.50/0

2. Experimental

2.1. Sample preparation

$Mo(CO)_6$ was engaged in NaY by a chemical vapor deposition (CVD) method according to the literature [6,7]. Briefly, NaY zeolite (Tosoh HSZ-300NAA, Si/Al = 2.6) was mounted in a sample cell made of stainless steel with two Kapton windows and two valves. The zeolite was calcined at 723 K for 30 min in a flow of O_2 (20%)/He (80%) (50 $cm^3\,min^{-1}$), followed by evacuation at 723 K for 1 h. $Mo(CO)_6$ (Aldrich, >98%) was placed in a glass tube wrapped with Al foil in order to protect $Mo(CO)_6$ from photodecomposition. The cell was connected to the glass tube of $Mo(CO)_6$ and to a rotary pump. The NaY zeolite in the cell was exposed to $Mo(CO)_6$ vapor for 24 h at room temperature. The Mo amount in the sample was 3.0 wt% determined by ICP (inductively coupled plasma) spectrometry (Seiko SPS7000) and the sample thickness was regulated so that the edge jump was ca. 0.5. The DXAFS spectra were measured during the temperature-programmed decarbonylation of the molybdenum species at a heating rate of 5 K min^{-1} under continuous evacuation.

2.2. DXAFS analysis

DXAFS measurement and analysis are described in a previous paper [25]. Briefly, DXAFS measurements at the Mo K-edge were carried out using synchrotron radiation at BL-9C of KEK-PF. A triangle-shaped Si(311) bent crystal was used to focus the polychromatic X-ray beam. The crystal was bent with a radius of curvature of 4000 mm. The distance between the crystal and the focus was approximately 380 mm and the horizontal width of the focus was ca. 0.5 mm. The sample was placed at the focus position. The diverging X-rays were detected by a photodiode array. Energy calibration was carried out using a spectrum of Mo foil. The channels of the photodiode array were correlated to the X-ray energy with a second-order polynomial. The energy range was 19800–20450 eV. Each spectrum was recorded in 1.5 s acquisition time (300 ms × 5 scan).

The spectra at Mo K-edge were analyzed by the UWXAFS package [26]. After background subtraction using AUTOBK [27], k^3-weighted EXAFS functions were Fourier transformed into R-space and fitted in the R-space. The k range of the Fourier transformation and the R range used for fitting were 30–90 nm^{-1} and 0.11–0.32 nm, respectively. The backscattering amplitudes and phase shifts were calculated by the FEFF8 code [28].

Conventional EXAFS measurements at the Mo K-edge were carried out using the Si(311) channel-cut monochromator at BL-10B of KEK-PF. The spectra at Mo K-edge were measured at 293, 473 and 623 K during the decarbonylation of $Mo(CO)_6$/NaY under vacuum and analyzed by the UWXAFS package. The k range of the Fourier transformation and the fitting R range were 30–145 nm^{-1} and 0.12–0.32 nm, respectively.

3. Results and discussion

Figure 1 shows a series of Mo K-edge X-ray absorption spectra for $Mo(CO)_6$/NaY during the temperature-programmed decarbonylation under vacuum at a heating rate of 5 K min^{-1} in the temperature range 293–623 K. Significant changes in the XANES spectra were observed at 400 and 500 K. The series of X-ray absorption spectra suggests that there is an intermediate species at ca. 400–550 K. To confirm this idea, the XANES spectra (19950–20050 eV) were fitted by a linear combination of those measured at 293,

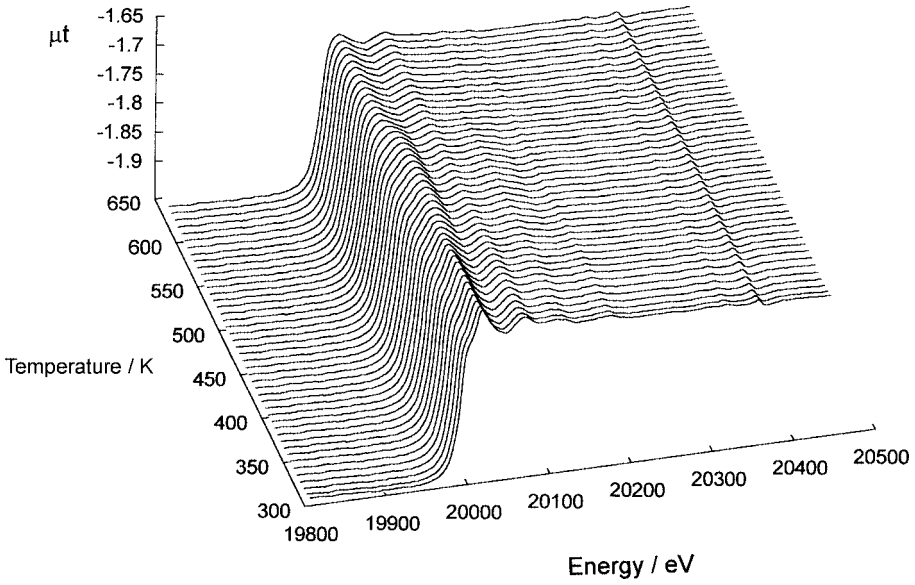

Figure 1. Energy-dispersive X-ray absorption spectra at Mo K-edge for $Mo(CO)_6$/NaY during the decarbonylation under vacuum from 293 to 623 K. The heating rate and the data acquisition time are 5 K min^{-1} and 1.5 s, respectively.

473 and 623 K, which represented the initial, intermediate, and final Mo species, respectively, as presented in the following formula:

$$X_{\mathrm{obs}} = c_0 X_0 + c_1 X_1 + c_2 X_2,$$

where X_{obs}, X_0, X_1 and X_2 represent observed XANES spectrum and XANES spectra of the initial, intermediate and final species, respectively, and c_0, c_1 and c_2 stand for the coefficients for X_0, X_1 and X_2, respectively.

Figure 2 shows c_0, c_1, c_2, $c_0 + c_1 + c_2$ and R_{f} as functions of decarbonylation temperature. The values of the sum of the coefficients $c_0 + c_1 + c_2$ were close to unity, and R_{f} was less than 0.8% in the whole temperature range, which indicate that the fitting was done properly. The value of c_0 began to decrease at 320 K and got to zero at 440 K, accompanied with an increase of c_1, and the value of c_1 began to decrease at 490 K and got to zero at 580 K, accompanied with an increase of c_2. The XANES analysis suggests that a stable intermediate species exists between 440 and 490 K. As the coefficient for the intermediate species was unity in the wide temperature range 440–490 K, it is reasonable that only the intermediate species exists in this temperature range. The idea is also supported by the fact that the conventional EXAFS spectrum after decarbonylation at 473 K was fitted well with three short Mo–CO and three Mo–O_{L} ligands. If the sample were a mixture of different Mo species, additional bondings would have been required to fit the data and the R_{f} should have been larger. Thus, the ratios of the species are equal to the coefficients obtained by the XANES analysis because the XANES spectra used as references were for single species.

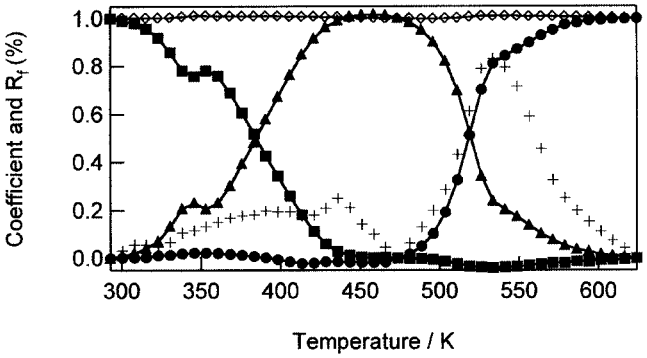

Figure 2. The coefficients (c_0, c_1 and c_2) for initial (■), intermediate (▲) and final (●) Mo species as a function of decarbonylation temperature as well as the sum of the coefficients (◇) and the residual factors R_{f} (+). The XANES spectra measured at 293, 473 and 623 K were used as reference spectra for the initial, intermediate and final species, respectively.

Figure 3 shows Fourier-transformed k^3-weighted EXAFS functions of $Mo(CO)_6$/NaY during the temperature-programmed decarbonylation. Phase shift correction is not carried out in these spectra. Mo–C and Mo–(C)–O peaks were observed at 0.15 and 0.27 nm (phase shift uncorrected), respectively. The intensity of these peaks began to decrease at 320 K, and decreased until 400 K. Above 400 K, Mo–C and Mo–(C)–O peaks shifted to 0.14 and 0.25 nm (phase shift uncorrected), respectively, and the intensity of these peaks increased. At 530 K, Mo–C and Mo–(C)–O peaks disappeared and two peaks at 0.15 and 0.27 nm (phase shift uncorrected) appeared together with an artificial peak at 0.089 nm caused by background subtraction.

At 293 K, two peaks were fitted by Mo–C and Mo–(C)–O contribution. The coordination numbers (CNs) of Mo–C and Mo–(C)–O bonds in the Mo carbonyls were set to an equal value. Calculated Debye–Waller factors from the EXAFS data measured at several temperatures were used. The value of the threshold energy (ΔE_0) was fixed at a certain value and the same value was used in the analysis of whole data. The value was determined so that the average residual factor got minimum. At 340 K, the peaks were fitted by Mo–O as well as Mo–C and Mo–(C)–O contribution. At 400 K, two peaks were fitted by five shells; Mo–O, Mo–C, Mo–(C)–O, short Mo–C and short Mo–(C)–O. In this case, the interatomic distances (R) for the carbonyl ligands

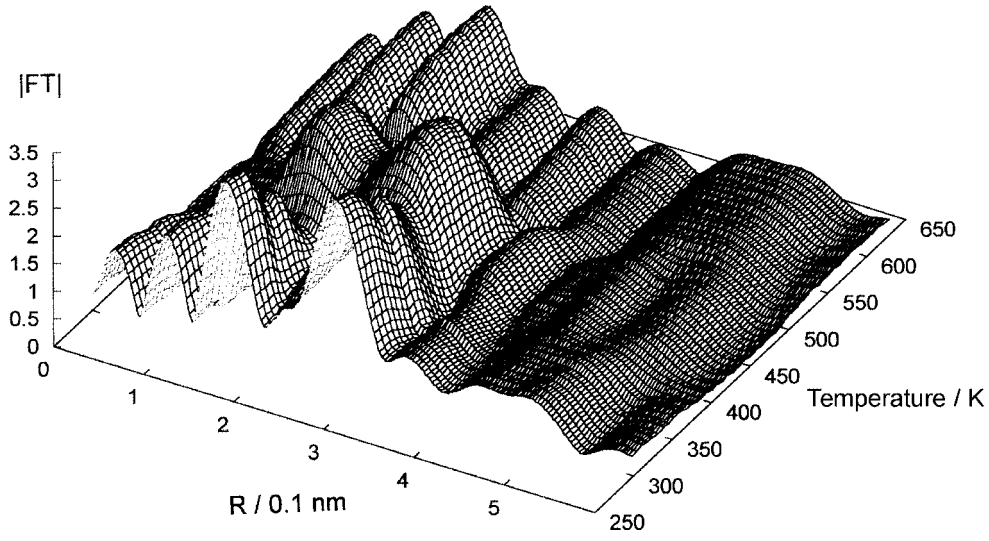

Figure 3. Fourier-transformed k^3-weighted EXAFS functions obtained from the spectra in figure 1.

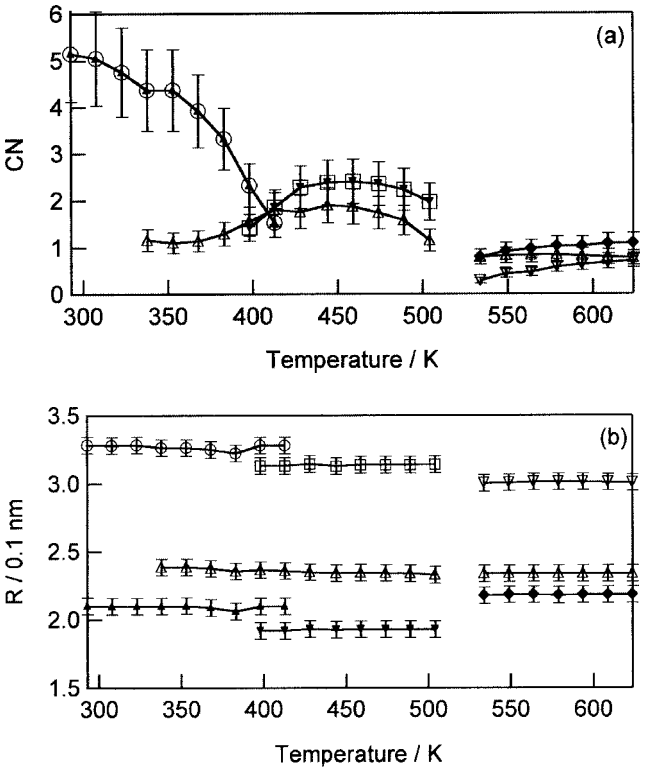

Figure 4. The coordination numbers (CN) (a) and bond distances (R) (b) as a function of decarbonylation temperature; (▲) Mo–C, (○) Mo–(C)–O, (△) Mo–O, (▼) short Mo–C, (□) short Mo–(C)–O, (▽) Mo–Mo and (♦) Mo–C.

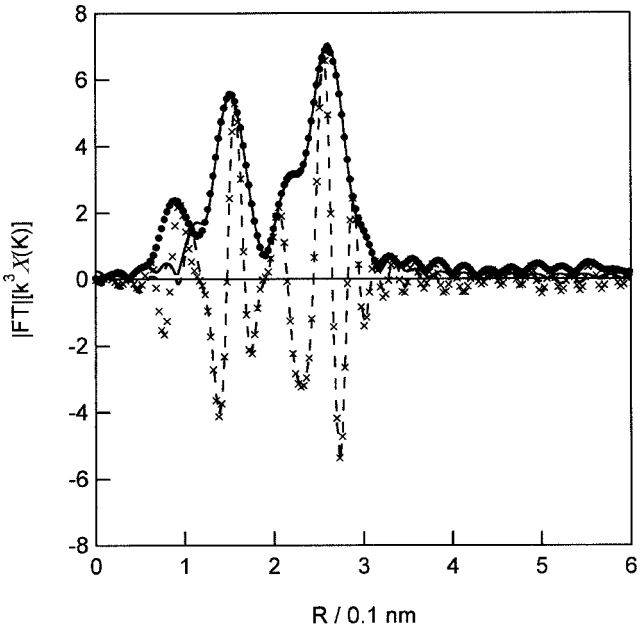

Figure 5. Fourier-transformed k^3-weighted EXAFS functions at Mo K-edge for the intermediate species in NaY. (•), (×), (—) and (- - -) represent observed EXAFS, its imaginary part, calculated EXAFS, and its imaginary, respectively.

were fixed because the number of free parameters should be smaller than the number of independent parameters calculated from the Niquest law (eight in this case) [29]. Above 430 K, the peaks were fitted by Mo–O, short Mo–C and short Mo–(C)–O contributions. At 530 K, two peaks at 0.15 and 0.27 nm (phase shift uncorrected) were fitted by Mo–Mo, Mo–C and Mo–O contributions.

Figure 4 shows the CN and R determined by the curve fitting analysis as a function of temperature. At 293 K, the bond distances of Mo–C and Mo–(C)–O were 0.210 and 0.328 nm, respectively. The CNs of these bonds were 5.1, which indicates that the $Mo(CO)_6$ structure is intact in the NaY [6,7]. The CNs of Mo–C and Mo–(C)–O bonds decreased between 320 and 420 K.

There are two possibilities for the first step of the decarbonylation at 300–440 K. One possibility is that the decarbonylation proceeds step by step through $Mo(CO)_x$ ($x = 4$ or 5) species. The other possibility is that three CO ligands desorb simultaneously from $Mo(CO)_6$, and only the initial species and the stable intermediate species exist, where the ratio of the "intermediate" species to the "initial" species increases with decarbonylation. The result of the XANES analysis suggests the latter possibility, though the first possibility is not completely excluded. As shown in figure 2, the XANES spectra observed between 300 and 440 K are represented well by the linear combination of those of the initial and intermediate species with small residual factors (less than 0.3%), without taking other species such as $Mo(CO)_5$ and $Mo(CO)_4$ into account. The result indicates that $Mo(CO)_6$ and $Mo(CO)_3(O_L)_3$ are the only species existing in this temperature range and the change in the XANES spectra is attributed to the change of the relative concentration of the $Mo(CO)_6$ and $Mo(CO)_3(O_L)_3$ species, because the XANES spectra of $Mo(CO)_6$ and $Mo(CO)_3(O_L)_3$ cannot be reproduced by a linear combination of $Mo(CO)_5$ and $Mo(CO)_4$. The latter possibility is also supported by the fact that the coefficients for the initial and intermediate species behaved in a similar way to the CNs of the Mo carbonyl species with longer and shorter Mo–CO distances, respectively. The normalized CNs by the ratio of these species were almost constant at six (initial species) and three (intermediate species), which implies that the change in the XANES spectra can be explained by the change in the ratio of the initial and intermediate species.

In the temperature range 430–480 K, short Mo–C and short Mo–(C)–O were observed at 0.193 and 0.314 nm, respectively. The CNs of these bonds were 2.4. The decrease of these bond distances may be attributed to the extension of the d $\rightarrow$ π^* back-donation [17]. A Mo–O bond was observed at 0.234 nm (CN 1.9). In the temperature range 430–480 K, the DXAFS data can be fitted without Mo–Mo contribution, which may exclude the possibility of Mo dimer subcarbonyl species. In order to reveal the structure of this stable intermediate species exactly, the spectrum of conventional EXAFS was measured at 293 K after decarbonylation at 473 K. Figure 5 shows the Fourier-transformed k^3-weighted EXAFS function as well as the curve fitting results for the intermediate species obtained by the conventional EXAFS measurement after decarbonylation at 473 K. As shown in figure 5, the observed data

Table 1
Structural parameters for the molybdenum species in NaY during the course of temperature-programmed decarbonylation process, determined by conventional EXAFS.[a]

Abs.-scat.	CN	R (0.1 nm)	σ^2 ($\times 10^{-5}$ nm^2)
At 293 K ($\Delta E_0 = 0.9$ eV, $R_f = 3.0\%$)			
Mo–C	5.1 ± 0.7	2.06 ± 0.01	1.3
Mo–(C)–O	5.1 ± 0.7	3.24 ± 0.02	2.6
At 473 K ($\Delta E_0 = 1.9$ eV, $R_f = 1.6\%$)			
Mo–C	3.3 ± 0.4	1.92 ± 0.06	2.8
Mo–(C)–O	3.3 ± 0.4	3.09 ± 0.06	3.7
Mo–O	2.9 ± 1.0	2.31 ± 0.08	9.5
At 623 K ($\Delta E_0 = 2.2$ eV, $R_f = 3.1\%$)			
Mo–C	1.0 ± 0.3	1.95 ± 0.01	7.0
Mo–O	2.1 ± 1.0	2.05 ± 0.01	4.7
Mo–Mo	1.0 ± 0.3	2.78 ± 0.02	10.8

[a] The conventional EXAFS spectra were measured at 293 K after the decarbonylation.

were reproduced well by calculated EXAFS. Table 1 shows structural parameters for the Mo species decarbonylated at 293, 473 and 623 K obtained by the curve fitting analysis. When the sample was evacuated at 473 K, the CN of Mo–C and Mo–(C)–O decreased to 3.3 with decreasing Mo–C and Mo–(C)–O distances. In addition, Mo–O_L bonds were observed at 0.231 nm (CN 2.9). On the basis of the conventional EXAFS data, it is concluded that the stable monomer intermediate species $Mo(CO)_3(O_L)_3$ (O_L: zeolite framework oxygen atom) are formed during the decarbonylation of $Mo(CO)_6$/NaY up to 473 K. The CNs for Mo–C and Mo–(C)–O calculated from the conventional EXAFS were 3.3 and 3.3, while those from the DXAFS were 2.4 and 1.9, respectively. The difference in the CNs obtained from the conventional EXAFS and the DXAFS may be attributed to the different measurement temperatures. The data of the conventional EXAFS were measured at 293 K, while those of the DXAFS were measured at the reaction temperatures 400–500 K. We think that the difference in measuring temperature is responsible for the difference in the CNs. CNs are apt to be underestimated when the spectra are measured at high temperatures because of unharmonic distribution of inter-atomic distances.

At 530 K, the peak of Mo–C and Mo–(C)–O disappeared and the spectra above 530 K were well fitted by Mo–O, Mo–Mo and Mo–C. According to the curve fitting of the conventional EXAFS after the decarbonylation at 623 K, the CNs (and bond distances) of Mo–O, Mo–Mo and Mo–C were 2.1 (0.205 nm), 1.0 (0.278 nm) and 1.0 (0.195 nm), respectively, as shown in table 1. The structure after the decarbonylation was Mo oxycarbide dimer species, $Mo_2(C)O_x$ [6,7]. The results in figures 2 and 4 suggest that the transformation of $Mo(CO)_6 \rightarrow Mo(CO)_3(O_L)_3$ proceeded gradually and it took over 100 K and that the transformation of $Mo(CO)_3(O_L)_3 \rightarrow Mo_2(C)O_x$ proceeded readily and completed in the temperature range of 50 K.

In summary, the DXAFS study reveals that $Mo(CO)_3(O_L)_3$ is the intermediate to form $Mo_2(C)O_x$ and that $Mo(CO)_6$ in NaY zeolite changes stepwise during the decarbonylation, $Mo(CO)_6 \rightarrow Mo(CO)_3(O_L)_3 \rightarrow Mo_2(C)O_x$. According to the XANES analysis and the curve fitting analysis of the DXAFS spectra, $Mo(CO)_6$ in NaY begins to change to $Mo(CO)_3(O_L)_3$ at 320 K. The $Mo(CO)_3(O_L)_3$ is a stable subcarbonyl species between 440 and 490 K. Mo dimer subcarbonyl species were not detected. $Mo(CO)_3(O_L)_3$ species changes to $Mo_2(C)O_x$ at 500–550 K. The present study demonstrates that the DXAFS technique is powerful and useful to monitor the dynamic structure change in metal carbonyl species during the temperature-programmed decarbonylation process in a 1 s time scale.

Acknowledgement

This work has been supported by CREST (Core Research for Evolutional Science and Technology) of Japan Science and Technology Corporation (JST). The XAFS measurements were done by the approval of the PAC committee (proposal No. 99G237).

References

[1] Y. Iwasawa, in: *Proc. 11th Int. Congr. on Catalysis*, Stud. Surf. Sci. Catal., Vol. 101 (Elsevier, Amsterdam, 1996) p. 21.
[2] Y. Iwasawa, Catal. Today 18 (1993) 21.
[3] Y. Iwasawa, Adv. Catal. 35 (1987) 187.
[4] G.A. Ozin and C. Gil, Chem. Rev. 89 (1989) 1749.
[5] C. Bremard, Coord. Chem. Rev. 178–180 (1998) 1647.
[6] T. Shido, K. Asakura, Y. Noguchi and Y. Iwasawa, Appl. Catal. A 194 (2000) 365.
[7] K. Asakura, Y. Noguchi and Y. Iwasawa, J. Phys. Chem. B 103 (1999) 1051.
[8] G.A. Ozin, S. Ozkar and R.A. Prokopowicz, Acc. Chem. Res. 25 (1992) 553.
[9] Y. Okamoto, A. Maezawa, H. Kane, I. Mitsushima and T. Imanaka, J. Chem. Soc. Faraday Trans. I 84 (1998) 851.
[10] Y. Okamoto, H. Kane and T. Imanaka, Chem. Lett. (1988) 2005.
[11] S. Abdo and R.F. Howe, J. Phys. Chem. 87 (1983) 1713.
[12] S. Ozkar, G.A. Ozin, K. Moller and T. Bein, J. Am. Chem. Soc. 112 (1990) 9575.
[13] Y. You-Sing and R.F. Howe, J. Chem. Soc. Faraday Trans. I 82 (1986) 2887.
[14] A. Maezawa, H. Kane, Y. Okamoto and T. Imanaka, Chem. Lett. (1988) 241.
[15] Y. Okamoto, A. Maezawa, H. Kane and T. Imanaka, J. Catal. 112 (1988) 585.
[16] S. Abdo and R.F. Howe, J. Phys. Chem. 87 (1983) 1722.
[17] A. Kazusaka and R.F. Howe, J. Mol. Catal. 9 (1980) 183.
[18] A. Brenner and R.L.J. Burwell, J. Am. Chem. Soc. 97 (1975) 2565.
[19] A. Brenner and R.L.J. Burwell, J. Catal. 52 (1978) 353.
[20] Y. Iwasawa, ed., *X-ray Absorption Fine Structure for Catalysts and Surface* (World Scientific, Singapore, 1996).
[21] Y. Okamoto, T. Imanaka, K. Asakura and Y. Iwasawa, J. Phys. Chem. 95 (1991) 3700.
[22] T. Matsushita and R.P. Phizackerley, Jpn. J. Appl. Phys. 20 (1981) 2223.
[23] A.M. Flank, A. Fontaine, A. Jucha, M. Lemonnier, D. Raoux and C. Williams, Nucl. Instrum. Methods 208 (1983) 651.

[24] E. Dartyge, A. Fontaine, A. Jucha and D. Sayers, *EXAFS and Near Edge Structure III* (Springer, Berlin, 1984) p. 472.
[25] A. Yamaguchi, T. Shido, Y. Inada, T. Kogure, K. Asakura, M. Nomura and Y. Iwasawa, Catal. Lett. 68 (2000) 139.
[26] E.A. Stern, M. Newville, B. Ravel, Y. Yacoby and D. Haskel, Physica B 208 (1995) 117.
[27] M. Newville, P. Livins, Y. Yacoby, E.A. Stern and J.J. Rehr, Phys. Rev. B 47 (1993) 14126.
[28] A.L. Ankudinov, B. Ravel, J.J. Rehr and S.D. Conradson, Phys. Rev. B 58 (1998) 7565.
[29] E.A. Stern, Phys. Rev. B 48 (1993) 9825.